

ZDDP and MoDTC interactions and their effect on tribological performance – tribofilm characteristics and its evolution

A. Morina*, A. Neville, M. Priest and J.H. Green

School of Mechanical Engineering, The University of Leeds, Leeds, UK

Received 16 June 2005; accepted 29 January 2006; published online 11 November 2006

In this work, the interactions between two key additives in current lubricants (ZDDP and MoDTC) and the effect on tribofilm formation and tribofilm evolution under boundary lubrication are studied. The chemical and tribological characteristics of the tribofilms are probed using measurement of friction, wear and film characteristics. Tribofilms have been examined by energy dispersive X-ray analysis (EDX) and X-ray photoelectron spectroscopy (XPS). In order to investigate the morphology of the reaction films formed, atomic force microscopy (AFM) was used. In this work, for the first time, a link between a proposed MoDTC breakdown mechanism and MoDTC tribofilm characteristics, measured on experimentally derived tribofilms, is made.

KEY WORDS: additive interactions, ZDDP, MoDTC, tribofilm, tribochemistry

1. Introduction

A very important class of friction-reducing additives, used extensively in crankcase lubricant formulations, are the molybdenum-containing compounds such as molybdenum dialkyldithiocarbamate (MoDTC). The total additive package amount in the lubricant can be in the range of 5–25% [1] and the effectiveness of MoDTC in reducing friction is strongly affected by synergistic or antagonistic effects with other additives, especially zinc dialkyldithiophosphate (ZDDP). The ZDDP additive, besides having anti-oxidant properties, is known to be very effective in protecting the surfaces from wear under boundary lubrication conditions, and is an essential ingredient in the vast majority of current lubricant formulations [2]. Being the two key components in lubricants, understanding the interactions between ZDDP and MoDTC in tribological performance is therefore essential for achieving optimum performance.

It is reported that MoDTC reduces friction by forming a MoS₂-containing film on the tribological contact [3–8]. The layer-lattice structure of the molybdenum disulphide makes it possible for low friction to be achieved between the tribocouple components [9]. The C-based tribofilm contains a few percent of highly dispersed MoS₂ in the form of individual sheets of length less than 10 nm [8]. In the work by Grossiord *et al.* [8], the breakdown of the MoDTC molecule from a chemical point of view is proposed, as shown in figure 1. They suggest that the initial step towards MoS₂ formation is via electron transfer at the Mo–S chemical bond in MoDTC (figure 1a), leading to the formation of three

free radicals (figure 1b): one corresponding to the core of MoDTC and the other two to the chain ends. The third step is the core radical decomposition (figure 1c) into MoS₂ and MoO₂, which can oxidise in the presence of O₂, and the recombination of chain end radicals forming thiuram disulphides. This mechanism has still not yet been shown experimentally to happen in the tribological contacts. Proof of the mechanism being correct is based solely on the observation of MoS₂ on tribofilms when friction is reduced.

There are reports in the literature that show that MoDTC alone is not as effective in friction reduction as it is when used together with the ZDDP additive [10–12]. It is proposed that in the presence of a mixed MoDTC/ZDDP system, a two-step reaction occurs: first, a reaction between phosphate and iron oxide and second a reaction between the nascent iron surface and a sulphide species [13]. It is suggested that the two additives act separately, ZDDP producing the zinc phosphate glass on one hand and MoDTC producing both MoS₂ and MoO₃ on the other hand [14]. The elimination of MoO₃, and prevention of MoS₂ from oxidation, suggested to happen according to the hard and soft acid and base (HSAB) principle, were thought to be the reason why a combined MoDTC/ZDDP system is more effective in reducing friction compared to MoDTC alone.

Although a good picture of the final species formed when the MoDTC additive is used can be obtained from reviewing the work done by several groups, the reaction sequence by which MoDTC forms MoS₂ has not yet been proven. Also, the effect of ZDDP and operating conditions on the mechanism of MoS₂ formation from MoDTC, and vice versa, the effect of MoDTC on ZDDP tribofilm formation are still poorly defined.

*To whom correspondence should be addressed.
E-mail: A.Morina@leeds.ac.uk

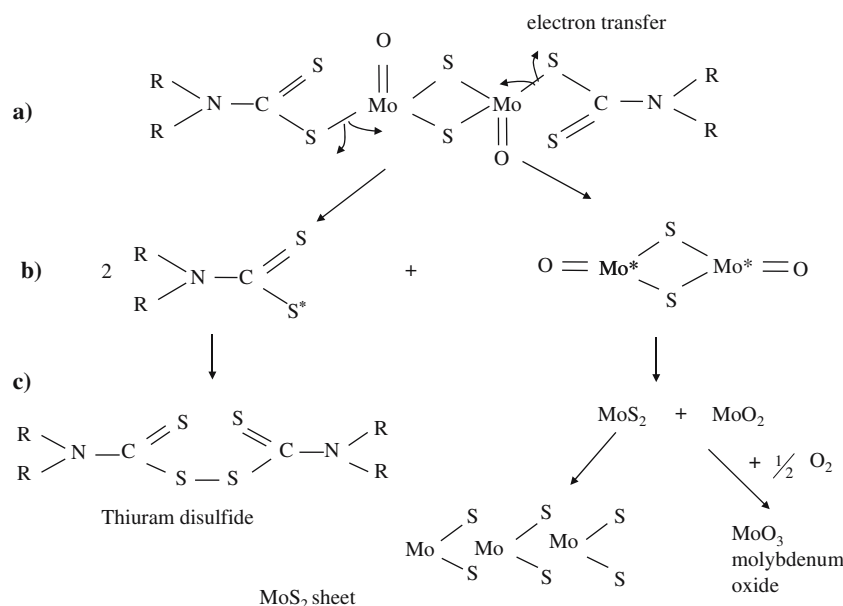


Figure 1. Molybdenum dialkyldithiocarbamate (MoDTC) decomposition chemical model [8].

In order to better understand the interactions between ZDDP and MoDTC, as principle additives in current engine lubricant additive packages, in this work model lubricants with only ZDDP and MoDTC, alone or combined, have been studied. The aim is to contribute to the large body of work on lubricant additives explaining how these additives function and the mechanism of their interactions. Understanding these mechanisms is very important for being able to blend lubricants which can offer optimum performance and also for introducing new additives with similar effectiveness but which are environmentally friendly. In this work, for the first time, a link between a proposed MoDTC breakdown mechanism shown in figure 1 and MoDTC tribofilm characteristics at various stages of its evolution is made.

2. Experimental

2.1. Tribological experiments

A reciprocating pin-on-plate apparatus is used in this work, and was instrumented to measure friction force via a bi-directional load cell with measuring range from 0 to 58.8 N with combined error of ± 0.0037 N. Combined error is an envelope of several errors such as non-linearity, hysteresis and temperature effect on load cell sensitivity. In this apparatus the plate reciprocates under a loaded pin, producing a 10 mm wear scar, where the velocity follows a sinusoidal profile. Readings of the friction force were taken every 10 min for 2 s (120 points), which corresponds to two stroke cycles. An average of the 120 points gives the friction force, which is used to calculate the friction coefficient. The friction coefficient was then calculated and plotted as a function

of time for the duration of the test. The tests were replicated at least three times and a good repeatability (average ± 0.004) for the friction coefficient in the last hour of the test was recorded.

All the tests were performed in the boundary lubrication regime. The calculation of the dimensionless film parameter, the lambda ratio (λ) was based on the starting composite root mean square surface roughness (σ_{rms}). This parameter was used to describe the lubrication regime and was calculated using the Dowson and Hamrock minimum film thickness equation in [15] for an elastohydrodynamic point contact. The radius on the pin used was 40 mm. Loads of 50 N and 188 N were used which give initial maximum Hertzian pressures of 410 and 640 MPa, respectively. The tests were undertaken at sliding speeds of 0.02 m/s and 0.1 m/s. Lambda ratios were well under unity showing that the lubrication is in the boundary regime. All the tests were performed with the lubricant at 100 °C. The samples were immersed for around 10 min before the test started. During this time, the calibration of the load cell is done. The duration of tests was 30 min and 6 h.

A 2^4 factorial design experiment procedure was applied for this study to narrow the potentially important factors into those that are statistically important with a specified level of confidence. The factors studied in this paper are:

- load (A),
- ZDDP concentration (B),
- MoDTC concentration (C)
- sliding speed (D).

All factors are analysed at their high and low level as shown in table 1. For the purpose of statistical analysis,

Table 1.
Factors and their high and low levels used in testing procedure.

| Factors | | | | |
|---------|-----------------|-------------------|--------------------|----------------------------|
| Level | A = Load (N) | B = ZDDP (wt%) | C = MoDTC (ppm) | D = Sliding Speed (m/s) |
| Low | 50 | 0 | 0 | 0.02 |
| High | 188 | 1.2 | 250 | 0.1 |

at least two replicates of each test were conducted and 32 tests were performed. The results were statistically analysed using Analysis of Variance (ANOVA) [16]. This analysis is done using the results from 6-h tests and the average friction coefficient taken over the last hour of the test was used as the *response*. This method allows statistical significance of factor effects to be judged at a known level of risk on the basis of a quantitative criterion. An *effect* can be interpreted as the change in response as the factor changes from its low to its high level [16]. The factor effects can also be presented graphically, following the procedure below [17]:

1. Identifying the largest and smallest average responses obtained.
2. Drawing a vertical scale to include all of these values.
3. Drawing a horizontal line at the grand average value. Grand average value is the average value of all responses obtained from tests.
4. For each factor, plotting the average response value at the high level and also at the low level. Plotting one point directly over the other, so one point will be above the grand average line and other will be below and equidistant from the grand average line.
5. Labelling the points and connecting each pair of points by a vertical line. The larger the vertical line the larger the change in response when going from low level to high level of a factor is.

Samples from tests where the optimum friction performance was observed were then chosen for further analysis using surface analytical techniques.

2.2. Materials and lubricants

The material used in this study for pins and plates was iron-based traditional engine material. The components were manufactured from one batch of AISI 52100 alloy steel to original rig dimensions. The pins used were 20 mm in length and 6 mm in diameter and the ends of the pins were machined to a 40 mm radius of curvature. The rectangular plate measured $15 \times 6 \times 3 \text{ mm}^3$. The components were through-hardened to 60-64HRC. Surface finish tolerances were specified as $R_a = 0.15\text{--}0.2 \mu\text{m}$ in the direction of sliding. The contact pair were immersed in the lubricant to be tested. For each test, 3 ml lubricant was used.

Table 2.
Lubricants composition and designation.

| Designation | Lubricant |
|-------------|-------------------------------------|
| 001A | PAO6 |
| 002A | PAO6 + 1.2 wt% ZDDP |
| 003A | PAO6 + 250 ppm MoDTC |
| 004A | PAO6 + 1.2 wt% ZDDP + 250 ppm MoDTC |

The lubricants used are defined in table 2.

The base oil used was synthetic oil Polyalphaolefin (PAO6) of viscosity 31 cSt (mm^2/s) at 40 °C and 5.8 cSt (mm^2/s) at 100 °C. Incorporating the additives did not result in significant change of base oil viscosity.

3. Post-test surface analyses

Post-test surface analyses were performed on the *plate* wear scars produced after 6-h tests, which were done in conditions that gave optimum friction performance, identified with ANOVA results, using all lubricants and on wear scars produced after 30-min tests using 003A and 004A lubricants. Environmental scanning electron microscopy (ESEM) with an energy dispersive X-ray analysis (EDX) attachment and X-ray photoelectron spectroscopy (XPS) were used to chemically characterise the tribofilm formed, while the atomic force microscope (AFM) was used to characterise the physical topography of the tribofilm.

3.1. ESEM/EDX analysis

The Philips XL30 ESEM/EDX, used in this study, is fully equipped with a range of secondary electron (SE) and back-scattered electron (BSE) detectors. Corrections for atomic number, absorption and fluorescence (ZAF) are achieved through a virtual standard calibration routine. The SEM images are taken in high vacuum conditions and $300\times$ magnification. The SEM is operated at an accelerating voltage of 20 kV and a working distance of 10 mm. The EDX technique, giving elemental information, will not identify specific chemical species. In addition, it has a probing depth in excess of $1 \mu\text{m}$ and hence will probe the substrate composition as well as the tribofilm itself. XPS is therefore used to complement EDX to provide very surface sensitive ($\sim 5 \text{ nm}$) information by probing only the wear film and analysing the composition as a function of depth.

3.2. XPS analysis

XPS analyses were performed on the Scienta ESCA300 facility in Daresbury, UK. The instrument

employs a high power rotating anode and monochromatised AlK α X-ray source. A large, seven crystals, double focusing monochromator focuses the X-rays to a line image, $6 \times 0.5 \text{ mm}^2$, on the sample, which is then focused in the middle of the wear scar in an area of $400 \times 300 \text{ }\mu\text{m}^2$. The binding energy of 284.8 eV for adventitious C is used as a reference for charge correction. The calibration of the binding energy scale is done by using as a reference the 4f_{5/2} and 4f_{7/2} lines of Au with binding energies of 87.64 and 83.98 eV, respectively. Prior to XPS analysis, the excess lubricant was drained from the surface and then the surface was immersed in heptane for about 2 s, in order to eliminate the residual lubricant. In a typical XPS analysis, a survey scan is obtained first in order to identify elements present, and then long scans of the selected peaks are obtained in order to determine a more comprehensive picture of the chemical composition. Acquisition conditions for the survey spectra were 300 eV pass energy, 2.9 mm slit size and 1.0 eV step interval. For the region spectra, the acquisition conditions were 300 eV pass energy, 2.9 mm slit size and 0.05 eV step interval. Under these conditions, the instrument resolution is 1.3 eV [18]. All the spectra were acquired in spatial mode. Chemical analyses as a function of depth were performed. Ar ion etching at 2 kV energy was done to facilitate this.

CasaXPS software [19] was used for performing the curve fitting procedures on XPS peaks obtained. The data obtained were compared with standard spectra and with the tabulated spectra from references [20–22]. Peak area ratio, difference between binding energies of the doublets and full width half maximum (FWHM) were constrained in order to obtain information with the most appropriate chemical meaning [18]. For example for the curve fitting of the S 2p doublet, the peak area ratio between 2p_{3/2} and the 2p_{1/2} was fixed to 2:1, in accordance with spin–orbit coupling. The two peaks of the S 2p doublet are separated between each other by 1.18 eV [20] and their FWHM is set to 1.7 eV. The value of FWHM of XPS peaks obtained in this work was convolution of analyser resolution [18] and of natural FWHM of the peak [20]. Although the FWHM values obtained from reference [20] were obtained using a different analyser and different slit size/pass energy to those used in the present work, their instrument resolution was undoubtedly rather small compared with that of the present work. Hence it is valid to use, for curve fitting purposes, FWHMs obtained by addition in quadrature of the linewidths [20] with the ESCA300 instrument resolution under the conditions used (1.3 eV).

All fitted spectra underwent a linear background subtraction, using limits spanning the entire analysed region. A Gaussian–Lorentzian (GL(30)) product function component line-shape was found to provide a satisfactory fit to the data from the Scienta instrument. Quantitative analysis was performed utilising peak area

sensitivity factors. A standard set of sensitivity factors held within the ESCA300 data analysis software have been used. These factors will vary with pass energy and lens mode, but in this study the quantification results are mainly given in a comparative mode between different tribofilms making the use of these factors acceptable.

3.3. AFM analysis

Atomic force microscopy (AFM) was used to probe the micro and nano-metric features of the surface wear film after the tribological tests. The scanning probe microscope (SPM) used in this work was a Topometrix TMX 2000 Explorer (TM Microscopes). The scannerhead has a maximum scan range in x , y , z direction of $100 \times 100 \times 8 \text{ }\mu\text{m}^3$, respectively. Scanning was carried out in contact mode with a Si₃N₄ cantilever, with a nominal spring constant of 0.03 Nm^{-1} . Constant force was employed by the cantilever during scanning with a set point in the range of 30 nA (force is related to the detector current). All images were obtained in ambient conditions.

3.4. Wear measurements

The wear factors are calculated from the wear scar diameter *on the pin*. Considering that the surface analyses are performed on the plate wear scars, measuring wear from the pins' wear scar was a compromise necessary to be taken because of the inability to accurately measure the small wear values on the plates. The wear calculated from pins' wear scar is used to indicate the lubricant effectiveness in wear reduction in the overall lubricating system.

4. Results

The work reported in this paper has two principal objectives. First, to understand the effect of additive–additive interactions (ZDDP and MoDTC) on tribological performance and film formation characteristics, and second to understand the sequence of processes involved in tribofilm formation which will then define tribofilm evolution. Following the development of the film characteristics as a function of time enables information to be accessed which will address the second objective.

4.1. Experimental design and statistical analysis – ANOVA

In figure 2, the output from the experimental design tests analysis is presented. Only factors showing a significant effect (based on 95% level of confidence) on friction and the limits at their high and low levels are shown.

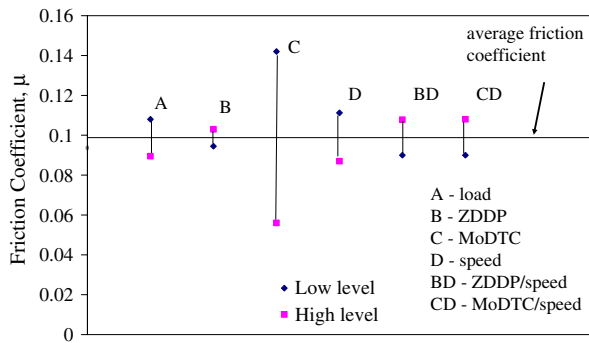


Figure 2. Factors with significant effects on friction, defined with 95% confidence from ANOVA statistical analysis.

It can be seen that, as expected, the factor which has the most significant effect on friction is the concentration of MoDTC additive. However, the experimental design highlights other potentially important factors and interactions that are not intuitive. After MoDTC, the factors which most significantly influence friction in descending order are:

- Load
- Concentration of ZDDP
- Interaction between ZDDP and speed
- Interaction between MoDTC and speed
- Speed

Statistically, the effect of the interactions between ZDDP and MoDTC on friction was found not to be significant. This will be discussed in detail later.

After analysing the significant interaction effects on friction, it can be concluded that the lowest friction will be reached when tests are done with a low level of ZDDP, a high level of speed and a high level of MoDTC. It could also be seen that when MoDTC is at its high level, speed does not have any effect on friction. So, the conditions, from the ones analysed, which gave lowest friction are 003A lubricant, 188 N and 0.1 m/s. In the wear scars produced by testing four different lubricants in these conditions, 188 N load, 0.1 m/s speed, testing temperature 100 °C and testing time 6 h, a full chemical analysis is undertaken to assess the tribofilm characteristics.

4.2. Tribological performance – friction and wear

Figure 3 shows the friction traces as a function of time from tests performed under the conditions which gave optimum friction identified in the previous section.

As in our previous work [23], from the friction results (figure 3) it can be seen that ZDDP presence in the base oil as the sole additive increases friction (comparison between 001A and 002A). It can also be seen that the presence of MoDTC in the base oil (i.e. 003A and 004A lubricants) reduced friction coefficient to 0.045–0.055.

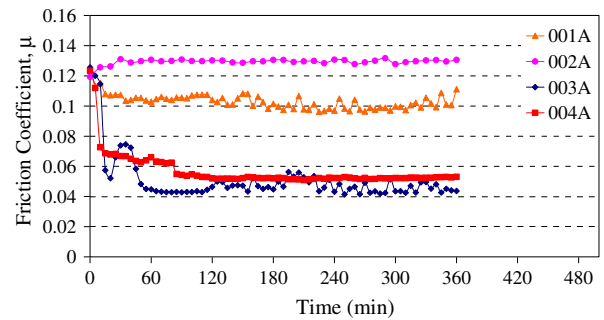


Figure 3. Friction traces from the tests where lubricants 001A, 002A, 003A and 004A were used.

The drop in friction when MoDTC is used alone (003A) is interesting since in several reports [10–12] it is shown that MoDTC can be highly effective as a friction reducing additive only in the presence of ZDDP. This has been shown not to be the case, although the friction response is much more stable when ZDDP is present.

In figure 4, the wear factors are shown. The wear measured on the plate samples was too small to be able to measure a clear distinction between lubricants hence wear calculated from pins' wear scar is used to indicate the lubricant effectiveness in wear reduction in the overall lubricating system. As expected the highest and lowest wear was experienced, respectively, in tests where 001A and 002A lubricants were used. Compared to 001A, 003A was also shown to reduce wear suggesting that in addition to friction-reducing properties MoDTC has also some anti-wear properties. This has also been observed in the literature [3, 12].

4.3. Tribofilm characteristics

4.3.1. SEM – comparison of three lubricants (002A, 003A and 004A)

A typical SEM image taken from the wear scar on plate produced with 002A lubricant is shown in figure 5. No significant difference, depending on the lubricant used could be seen. From the wear scar presented in

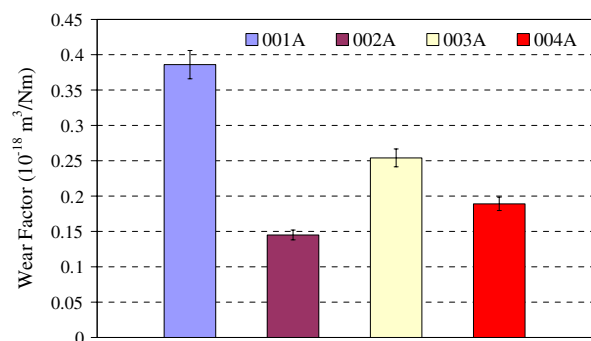


Figure 4. Wear coefficients from the tests where lubricants 001A, 002A, 003A and 004A were tested in 6 h tests.

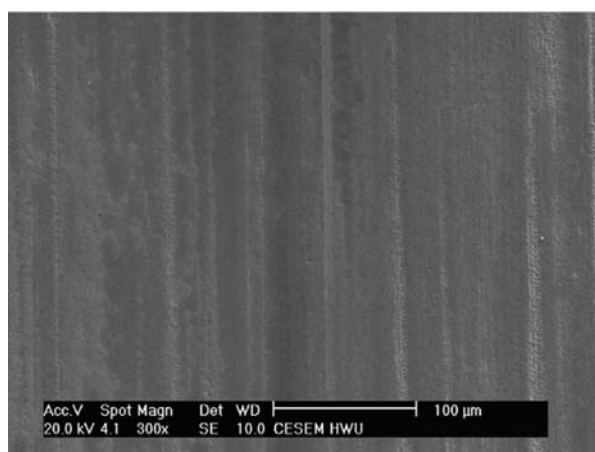


Figure 5. SEM image taken from the wear scar in the plate produced using 002A lubricant in 6 h test.

figure 5, it can be seen that mild wear has occurred which resulted in primarily flattening of asperities, agreeing with the low wear coefficient values of less than $4 \times 10^{-19} \text{ m}^3/\text{Nm}$ measured on the pin.

EDX analysis was taken from an area of $500 \times 400 \mu\text{m}^2$ at three different positions on each wear scar and similar chemical compositions with standard deviation of 10% were shown from area to area. In table 3, the representative chemical composition of the tribofilms analysed is shown where it can be seen that the P and Zn amounts change depending on whether MoDTC is used together with ZDDP (004A lubricant) or whether the ZDDP additive is used alone in the base oil (002A lubricant). This suggests that Zn phosphate

Table 3.

Tribofilm composition in wt% measured using EDX on the plates wear scar after 6 h tests.

| | EDX (wt%) | | | | | | | | | |
|------|-----------|-----|-----|------|-----|-----|-----|-----|-----|-----|
| | P | S | Zn | Fe | O | C | Cr | Si | Mn | Mo |
| 002A | 1.2 | 0.5 | 2.4 | 83.8 | 5.9 | 0 | 4.0 | 0.5 | 1.6 | – |
| 003A | – | 0.6 | – | 80.5 | 5.0 | 3.4 | 5.1 | 0.7 | 2.3 | 2.3 |
| 004A | 0.3 | 0.3 | 0.7 | 82.5 | 4.6 | 3.7 | 4.7 | 0.5 | 2.1 | 0.4 |

Table 4.

XPS quantification in at % of the tribofilms formed on the plates when 002A, 003A and 004A lubricants were tested in 6 h tests.

| | Etching time (min) | C 1s | O 1s | S 2p | P 2p | Fe 2p | Zn 2p | Mo 3d | N 1s |
|------|--------------------|------|------|------|------|-------|-------|-------|------|
| 002A | 0.5 | 14 | 51.7 | 5.5 | 14.9 | 4.9 | 9 | – | – |
| | 2 | 7.1 | 52.1 | 6.3 | 13.5 | 10.7 | 10.2 | – | – |
| | 5 | 5.5 | 46.8 | 6.9 | 12 | 19.5 | 9.3 | – | – |
| | 70 | 8.3 | 39.9 | 2.5 | 10.6 | 29.9 | 8.9 | – | – |
| 003A | 0.5 | 99.4 | 0 | 0.4 | – | 0 | – | 0.2 | 0 |
| | 5 | 91.2 | 2 | 2 | – | 0.6 | – | 2.1 | 2.2 |
| | 20 | 75.0 | 5.5 | 3.9 | – | 3.7 | – | 7.2 | 4.7 |
| 004A | 0.5 | 91.1 | 4.1 | 1.6 | 2.2 | 0 | 0.3 | 0.8 | 0 |
| | 2 | 74.9 | 8.1 | 3.1 | 4 | 0 | 2.1 | 1.7 | 3.7 |
| | 5 | 54.7 | 15.6 | 4 | 5.4 | 1.8 | 4.3 | 3.3 | 5.1 |
| | 20 | 31.8 | 17.1 | 3.2 | 4.2 | 18.5 | 3.7 | 4.7 | 8.7 |
| | 70 | 22.5 | 14.2 | 0 | 0 | 55.1 | 0 | 1.6 | 5.0 |

formation is affected by the presence of MoDTC. In this condition, a slight increase in the wear coefficient is observed which can be linked to the lower P and hence lower amount of phosphate glass formed on the wear scar. It can also be seen that the Mo amount is lower when 004A lubricant is used compared when 003A is used. This suggests that the presence of ZDDP in the lubricant also disrupts the formation of the Mo species from the tribochemical reaction of MoDTC. Both these observations prove that there is a “competition” between active species formed from ZDDP and MoDTC decomposition for wear scar surface.

4.3.2. XPS – comparison of three lubricants (002A, 003A and 004A)

In table 4, the quantification obtained from XPS of the tribofilms formed when 002A, 003A and 004A lubricants are used is shown.

- There are several important points from these analyses:
- A higher C amount is recorded, related to MoDTC presence in the lubricant.
- A different etching rate occurs, evident by the rate of change of C concentration with etching, depending on the additives used. This could be due to the different C-containing species formed.
- The oxygen concentration was seen to be lower in the tribofilms formed from MoDTC-containing lubricants. This does not mean that less O species are formed in these tribofilms since the high amount of C can cover the other species underneath.
- A nitrogen peak is found on tribofilms formed from 003A to 004A lubricants.

4.3.3. Effect of MoDTC on ZDDP tribofilm formation

In figure 6 and table 5, the species identified on samples when 002A and 004A lubricants were used, after applying the curve fitting procedure, are shown.

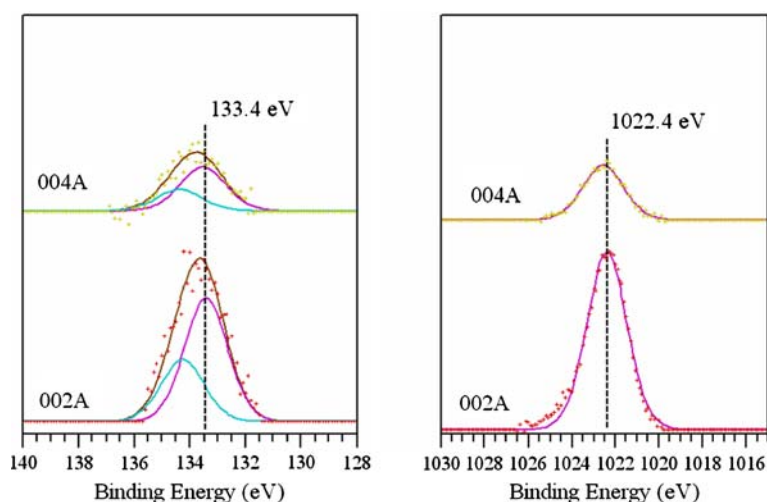


Figure 6. P 2p and Zn 2p peak curve fitting. These peaks were recorded in tribofilms formed on the plates from 002A and 004A lubricants in 6 h tests.

Table 5.

Curve fitting of S 2p and O 1s XPS peaks recorded in tribofilms formed on the plates from 002A and 004A lubricants in 6 h tests.

| Etching time (min) | 002A, S 2p | | | | 004A, S 2p | | | |
|--------------------|------------|-----------|----------|--------------------------------|------------|-----------|----------|----------|
| | BE (eV) | FWHM (eV) | Area (%) | Species | BE (eV) | FWHM (eV) | Area (%) | Species |
| 0.5 | 161.8 | 1.7 | 67.4 | Sulphide | 161.7 | 1.7 | 69.1 | Sulphide |
| | 162.5 | 1.7 | 32.6 | | 163.9 | 1.7 | 30.9 | |
| 2 | 161.8 | 1.7 | 100 | Sulphide | 161.8 | 1.7 | 84.4 | Sulphide |
| | | 1.7 | | | 163.7 | 1.7 | 15.6 | |
| 5 | 161.6 | 1.7 | 67 | Sulphide | 161.5 | 1.7 | 42.5 | Sulphide |
| | 162.5 | 1.7 | 33 | | 162.4 | 1.7 | 57.5 | |
| Etching time (min) | 002A, O 1s | | | | 004A, O 1s | | | |
| | BE (eV) | FWHM (eV) | Area (%) | Species | BE (eV) | FWHM (eV) | Area (%) | Species |
| 0.5 | 530.3 | 1.8 | 5.5 | Fe ₂ O ₃ | | | | |
| | 531.6 | 1.8 | 76 | NBO | 531.5 | 1.8 | 79 | NBO |
| | 533.1 | 1.8 | 19 | BO | 533.1 | 1.8 | 21 | BO |
| 2 | 530.3 | 1.8 | 15.2 | Fe ₂ O ₃ | | | | |
| | 531.6 | 1.8 | 73 | NBO | 531.5 | 1.8 | 81 | NBO |
| | 533.1 | 1.8 | 11.8 | BO | 533 | 1.8 | 19 | BO |
| 5 | 530.5 | 1.8 | 32.4 | Fe ₂ O ₃ | 530 | 1.8 | 6.2 | Oxide |
| | 531.7 | 1.8 | 59.7 | NBO | 531.7 | 1.8 | 81.2 | NBO |
| | 533.2 | 1.8 | 7.9 | BO | 533.2 | 1.8 | 12.6 | BO |

BE, FWHM and Area corresponds to binding energy, Full Width Half Maximum and the spectra area, respectively.

From figure 6, it can be observed that Zn and P binding energies, 1022.4 and 133.4 eV respectively, from both tribofilms are similar and correspond to a phosphate glass [21]. It should be appreciated that ZDDP tribofilms are not uniformly formed in the wear scar and they are formed in patches, as will be shown in AFM images of these films further in this study. In this work, the XPS analyses are done in an area of $400 \times 300 \mu\text{m}^2$, analysing several species at the same time which makes the problem of obtaining an exact phosphate structure even more complex. An important parameter for glass characterisation [24] is the ratio of bridging oxygen (P–O–P) to non-bridging oxygen (–P=O and P–O–Zn). Bridging oxygen (BO) and non-bridging oxygen (NBO)

values are determined from curve fitting of the O 1s XPS peak, shown in table 5.

From table 5, it can be observed that:

- S 2p binding energy, in general, corresponds to the sulphide region [20]. Some subtle differences in curve fitting components, due to the formation of different sulphides, were observed. The MoS₂, ZnS and FeS binding energies are near each other making it difficult to identify these species just by looking at the S 2p peak.
- No oxides were detected on the tribofilm surface formed when 004A lubricant is used in contrast with the one formed from 002A lubricant. The curve fitting

showed a reduction of NBO and BO and increase of oxides with etching.

4.3.4. Effect of ZDDP on MoDTC tribofilm formation

From the tribofilm quantification obtained with EDX, shown in table 3, it can be seen that more Mo species are detected when the 003A was used, compared to when 004A was used. This does not necessarily mean that more MoS₂ is formed since EDX gives only elemental information. From XPS quantification, shown in table 4, it can be seen that in the top tribofilm layers the amount of Mo is highest when 004A lubricant was used. The XPS peaks curve fitting procedure, shown in table 6, helps the Mo species in the tribofilm to be identified.

From these data, it can be summarised:

- Both tribofilms are found to have an upper carbon-rich phase, in agreement with the literature [14].
- MoS₂ was found on both tribofilms, and from friction results it could be seen that it is effective in friction reduction.
- A small amount of Mo was found to be as a Mo phosphate, in the tribofilm formed from 004A lubricant, showing that some interactions between Mo from MoDTC and P from ZDDP occur.
- The oxygen peak indicates that oxygen in the 003A and 004A tribofilms is found mainly as oxides. A small percentage of oxygen in 004A tribofilm can be found as a Mo phosphate.
- The S 2p peak of the 003A shows the formation of small amount of sulphates in the upper layer, in agreement with the observations from Kasrai *et al.* [10].
- A nitrogen peak was found on both tribofilms.

Table 6.

Curve fitting of the XPS peaks and the species that correspond to those binding energies recorded in tribofilms formed on the plates from 003A and 004A lubricants in 6h tests.

| Etching time (min) | 003A, Mo 3d | | | | 004A, Mo 3d | | | |
|--------------------|-------------|-----------|----------|------------------|-------------|-----------|----------|------------------|
| | BE (eV) | FWHM (eV) | Area (%) | Species | BE (eV) | FWHM (eV) | Area (%) | Species |
| 0.5 | 229.4 | 1.7 | 62.2 | MoS ₂ | 228.2 | 1.7 | 55 | MoS ₂ |
| | 232.2e | 1.7 | 18.4 | MoO ₃ | 229.6 | 1.7 | 19.8 | MoS ₂ |
| | | | | | 231.7 | 1.7 | 7 | MoO ₂ |
| | | | | | 233.3 | 1.7 | 2 | Mo phosphate |
| 5 | 228.4 | 1.7 | 59.5 | MoS ₂ | 228 | 1.7 | 64.8 | MoS ₂ |
| | 229.6 | 1.7 | 16.4 | MoS ₂ | 229.4 | 1.7 | 13.6 | MoS ₂ |
| | 232.2 | 1.7 | 19.2 | MoO ₃ | 231.8 | 1.7 | 11.6 | MoO ₂ |
| | | | | | 233.3 | 1.7 | 5.5 | Mo phosphate |
| 20 | 228.2 | 1.7 | 68 | MoS ₂ | 228 | 1.7 | 64.4 | MoS ₂ |
| | 229.6 | 1.7 | 18.3 | MoS ₂ | 229.6 | 1.7 | 14.7 | MoS ₂ |
| | 231.6 | 1.7 | 11.7 | MoO ₂ | 231.7 | 1.7 | 13 | MoO ₂ |
| | | | | | 233.4 | 1.7 | 6.6 | Mo phosphate |
| Etching time (min) | 003A, O 1s | | | | 004A, O 1s | | | |
| | BE (eV) | FWHM (eV) | Area (%) | Species | BE (eV) | FWHM (eV) | Area (%) | Species |
| 0.5* | | – | | – | 531.5 | 1.8 | 79 | NBO |
| 5 | | | | | 533.1 | 1.8 | 21 | BO |
| | 530.8 | 1.8 | 56 | Oxide | 530 | 1.8 | 6.2 | Oxide |
| | 532.8 | 1.8 | 44 | R–O | 531.7 | 1.8 | 81.2 | NBO |
| | | | | | 533.2 | 1.8 | 12.6 | BO |
| 20 | | | | | 530.2 | 1.8 | 24.4 | Oxide |
| | 530.7 | 1.8 | 56 | Oxide | 531.6 | 1.8 | 63 | NBO |
| | 532.3 | 1.8 | 44 | R–O | | | | |
| | | | | | 533.1 | 1.8 | 12.6 | BO |
| Etching time (min) | 003A, S 2p | | | | 004A, S 2p | | | |
| | BE (eV) | FWHM (eV) | Area (%) | Species | BE (eV) | FWHM (eV) | Area (%) | Species |
| 0.5 | 162.7 | 1.7 | 100 | Sulphide | 161.7 | 1.7 | 69.1 | Sulphide |
| | 169.7 | 1.7 | 100 | Sulphate | 163.9 | 1.7 | 30.9 | |
| 5 | 161.6 | 1.7 | 60 | Sulphide | 161.8 | 1.7 | 84.5 | Sulphide |
| | 163.1 | 1.7 | 40 | | 163.7 | 1.7 | 15.6 | |
| 20 | 161.8 | 1.7 | | Sulphide | 161.5 | 1.7 | 42.5 | Sulphide |
| | | | | | 162.4 | 1.7 | 57.5 | |

BO and NBO represent bridging oxygen and non-bridging oxygen, respectively, components of the oxygen peak. Although the detection of the Mo oxide after 0.5 min etching suggests that oxygen should be detected (at *), its amount is very small to be able to quantify it.

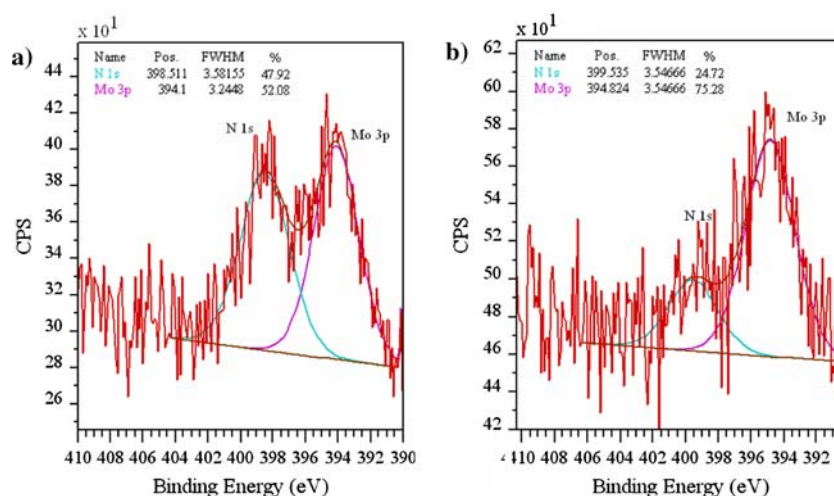


Figure 7. Curve fitting of the X-ray photoelectron spectroscopy (XPS) peak showing the presence of N 1s in the tribofilms formed by using (a) 004A and (b) 003A lubricants in 6 h tests.

Table 7.
N 1s peak curve fitting.

| Etching time (min) | 003A, 30 min, N 1s | | | 004A, 30 min, N 1s | | |
|--------------------|--------------------|-----------|---------|--------------------|-----------|---------|
| | BE (eV) | FWHM (eV) | Species | BE (eV) | FWHM (eV) | Species |
| 0.5 | No peak | | - | No peak | | - |
| 2 | 397.8 | 3.5 | Organic | 397.8 | 3.5 | Organic |
| | 400 | 3.5 | Species | 399.8 | 3.5 | Species |
| 5 | 397.6 | 3.5 | Organic | 394.0 | 3.5 | Mo 3p |
| | 400 | 3.5 | Species | 398 | 3.5 | Organic |
| | | | | 399.5 | | Species |
| Etching time (min) | 003A, 6 h, N 1s | | | 004A, 6 h, N 1s | | |
| | BE (eV) | FWHM (eV) | Species | BE (eV) | FWHM (eV) | Species |
| 0.5 | No peak | | - | No peak | | - |
| 5 | 394.4 | 3.5 | Mo 3p | 394.2 | 3.5 | Mo 3p |
| | 399 | 3.5 | Organic | 398.6 | 3.5 | Organic |
| | | | Species | | | Species |

The curve fitting of the XPS peaks at around 400 eV obtained after 5-min etching of 004A and 003A tribofilms formed in 6-h tests is shown in figure 7 and a summary of curve fitting results is given in table 7. The nitrogen peak on the wear scar was found to have binding energies in the region of BE = 397.6–400 eV. These binding energies correspond to species which can be generalised as R–N bonds [20].

4.4. Tribofilm evolution

The transient behaviour, shown in figure 3 as an abrupt drop in friction, is only seen when MoDTC-containing lubricants are used, either on its own or with ZDDP. Since the induction sliding distance before drop of friction was found to be relatively constant for tests at low and high sliding speeds, low sliding speed tests were used to analyse the tribofilm

evolution. This was done in order to give a reasonable time of 50 min prior to the friction drop. Tests were therefore performed at 30 min and 6 h to assess the evolution of the tribofilm.

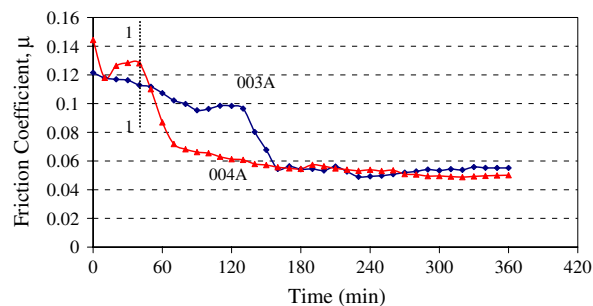


Figure 8. Friction trace when 003A and 004A lubricants were used. 1–1 shows the position in which the wear scar was chemically analysed.

Table 8.
XPS quantification for tests before and after the friction drop.

| Before the friction drop (30 min) | Etching time (min) | XPS quantification (at%) | | | | | | | |
|-----------------------------------|--------------------|--------------------------|------|------|------|-------|-------|------------|------|
| | | C 1s | O 1s | S 2p | P 2p | Fe 2p | Zn 2p | Mo 3d | N 1s |
| 003A | 0.5 | 85.8 | 9.5 | 0.9 | – | 3.8 | – | 0 | 0 |
| | 2 | 69.4 | 14.1 | 1.8 | – | 11.3 | – | 0 | 3.4 |
| | 5 | 51.4 | 18.3 | 1.3 | – | 22.3 | – | Small peak | 6.6 |
| 004A | 0.5 | 73.7 | 14.3 | 2.1 | 6.7 | 1.2 | 1.9 | 0 | 0 |
| | 2 | 54.6 | 24 | 2.6 | 8.9 | 2.4 | 3.7 | 0 | 3.8 |
| | 5 | 45.2 | 28 | 2.9 | 8.5 | 5.8 | 4.4 | 0.7 | 4.5 |
| | 20 | 17.9 | 31.9 | 3.3 | 9.5 | 27 | 4.3 | 1.1 | 4.9 |
| After the friction drop (6 h) | Etching time (min) | C 1s | O 1s | S 2p | P 2p | Fe 2p | Zn 2p | Mo 3d | N 1s |
| 003A | 0.5 | 99.4 | 0 | 0.4 | – | 0 | – | 0.2 | 0 |
| | 5 | 91.17 | 2 | 2 | – | 0.6 | – | 2.1 | 2.2 |
| | 20 | 75.03 | 5.5 | 3.9 | – | 3.7 | – | 7.2 | 4.7 |
| 004A | 0.5 | 91.1 | 4.1 | 1.6 | 2.2 | 0 | 0.3 | 0.8 | 0 |
| | 2 | 74.9 | 8.1 | 3.1 | 4 | 0 | 2.1 | 1.7 | 3.7 |
| | 5 | 54.7 | 15.6 | 4 | 5.4 | 1.8 | 4.3 | 3.3 | 5.1 |
| | 20 | 31.8 | 17.1 | 3.2 | 4.2 | 18.5 | 3.7 | 4.7 | 8.7 |

In figure 8, the friction response from tests with 003A and 004A lubricants from low sliding speed tests is shown.

A clear drop in friction coefficient was seen for both lubricants. The difference in length of induction time prior to friction drop, depending on the lubricant used, is investigated further by the authors [25]. In order to understand the tribofilm evolution, the tribofilms were chemically analysed before the drop of friction (the position 1–1 shown in figure 8) and results compared with

chemical analysis of the film formed at the end of test where the friction was low. In table 8, the XPS quantification of tribofilms formed using 003A and 004A lubricants before and after the friction drop is shown.

From the quantification, the following key points are observed:

- No significant amount of Mo species is found on the wear scar of the sample before the friction drop. The Mo 3d peak could be detected only after 5 min etching.

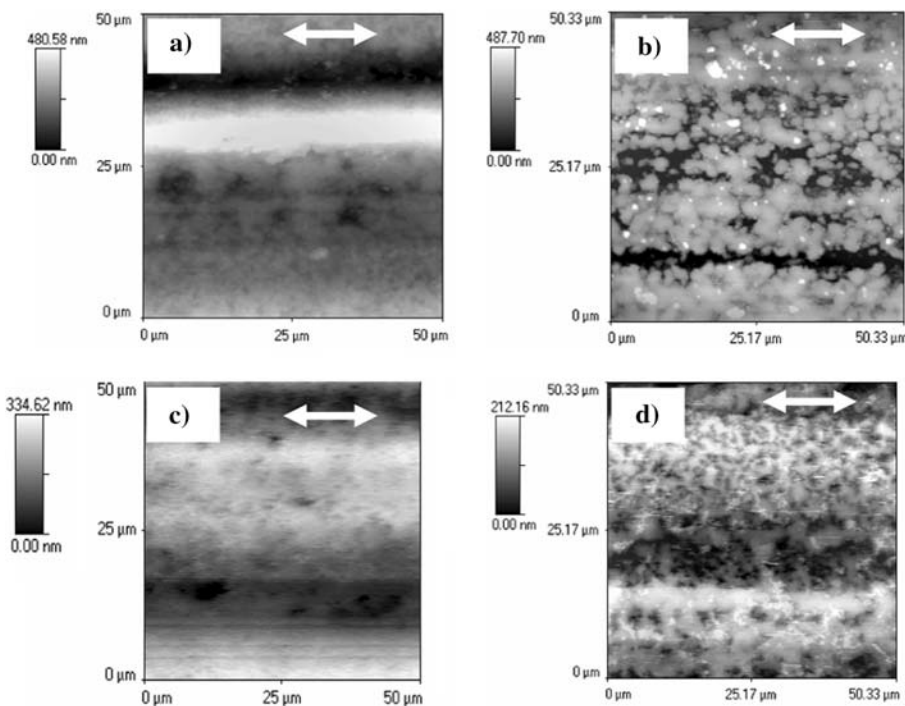


Figure 9. Tribofilms structures obtained using atomic force microscopy (AFM), (a) 003A, high friction, 30 min test; (b) 004A, high friction, 30 min test; (c) 003A, low friction, 6 h test; (d) 004A, low friction, 6 h test. The images are taken perpendicular to the sliding direction which is shown with arrows.

- An N 1s peak is detected on all the tribofilms.
- When 004A is used, before the friction drop, a tribofilm from the ZDDP additive was found to be formed. The curve fitting data of P and Zn peaks for this sample showed that a tribofilm similar to the one formed after the 6-h test is formed.
- The binding energy of S 2p peak detected in all four tribofilms (161.8 eV), corresponds to sulphides [20,26]. AFM images obtained in the wear scars, where high friction (30 min tests) and low friction (6-h tests) were observed, are shown in figure 9.

When 003A lubricant was used (comparing the images (a) and (c)), no distinctive change in film structure can be observed. This can be linked to the chemical composition, where in the top of both tribofilms, a C-rich layer is observed. Comparing images (b) and (d), it can be seen that the white structure is much more dense in the wear scars produced after longer tests (image (d)). The white structure, also observed in [27–29] is believed to be phosphate glass formed from the ZDDP additive.

5. Discussion

On the basis of the results presented, the film formed by using lubricants containing ZDDP and MoDTC additives, alone or combined, is now discussed.

From table 8, the presence of N and S in the tribofilm is very interesting and has not been previously reported. Both N and S are part of the MoDTC molecule (shown in figure 1a) and their presence on the wear scar suggests that a breakdown of MoDTC molecule has occurred before any reduction in friction is observed. However, absence of Mo in the tribofilms formed after 30-min tests implies that full transformation from MoDTC to MoS₂ on the surface has not occurred. The presence of N and S and no Mo gives an important clue to the breakdown mechanism of MoDTC and the subsequent reaction products developed at the surface. From curve fitting of the N 1s peak, shown in table 7 and figure 7, the binding energies suggested that N is at the surface as part of an organic species [30]. Formation of these species explains the high C amount detected by XPS in the wear scars produced with MoDTC-containing lubricants.

The identification of the N 1s peak with XPS was thought to be difficult due to the interference with Mo 3p peak [14]. In the above case, when the wear scars produced with MoDTC-containing lubricants after 30-min tests were analysed, molybdenum was not found in the wear scar making the N 1s peak obvious. Indeed, the N 1s peak is very close to Mo 3p peak but with careful curve fitting, all the peaks can be identified.

These findings correspond well with the mechanism proposed by Grossiard *et al.* [8]. One possible mechanism for N being at the surface is that the S in the

N-containing radical, formed from breakdown of MoDTC, reacts with the nascent surface according to the HSAB principle, since S²⁻ and metal atoms are known to be soft base and acid respectively, forming FeS_x and leaving the N part to deposit on the surface.

5.1. Effect of MoDTC on ZDDP tribofilm formation

Comparing the quantification of 002A and 004A, from table 4, which are lubricants with ZDDP and ZDDP/MoDTC respectively, it can be observed that the amount of Zn and P elements, known to be part of the ZDDP tribofilm are less on 004A compared to 002A, suggesting a thicker film is obtained when ZDDP is used alone (002A). This is in agreement with the EDX results shown in table 3. Formation of a thinner ZDDP tribofilm when MoDTC is present in the lubricant has also been reported by Muraki *et al.* [31] and is proposed to be due to the competitive adsorption between ZDDP and MoDTC.

Argon ion etching is performed on all samples under the same conditions (2 kV), and from the quantification analysis it is apparent that a different rate of element reduction occurs depending on whether MoDTC is present or not. When the film formed by using the 004A lubricant is analysed, the film was found to be C-rich, and after 70-min Ar⁺ etching no P, Zn or S were detected, while in the tribofilm formed from 002A lubricant, after the same etching time there was still a substantial tribofilm on the surface. The ZDDP tribofilm was completely removed after etching the 004A tribofilm. This suggests that when both additives are present in the lubricant, due to adsorption competition between additives at the sample surface the resulting ZDDP tribofilm thickness and homogeneity is reduced. In terms of tribological performance, a link between the amount of ZDDP additive elements (Zn, P and S percentage) found in the tribofilms and wear can be noticed. When 004A lubricant was used, less Zn, P and S was found in the tribofilm while wear was found to be higher.

The other question that arises is whether the presence of MoDTC additive changes the principal species in the ZDDP tribofilm. The binding energies of ZDDP elements found on the wear scar (figure 6 and table 5) show the formation of a phosphate glass [20,21], which is in agreement with the other work [24]. Detection of the S peak showed formation of sulphides whenever ZDDP was used with MoDTC or alone. To see the effect of MoDTC on ZDDP tribofilm formation, the characterisation of the phosphate glasses formed is necessary. An important parameter for glass characterisation is the ratio of bridging oxygen (P–O–P) to non-bridging oxygen (–P=O and P–O–Zn), which is equal to BO/NBO = $(n-1)/2(n+1)$ [24]. From this, the glass polymerisation number (n) can be calculated. In the cases where $n = 1$, the glass is an orthophosphate, $n = 2$ is a pyrophosphate and in the case that n is

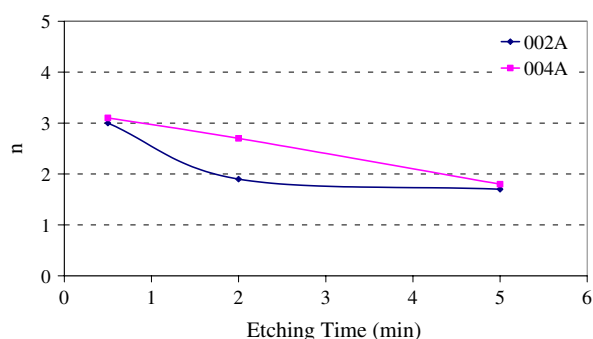


Figure 10. Phosphate glass polymerisation number as a function of tribofilm etching.

higher than 2 it is a metaphosphate [32]. BO and NBO values are determined from XPS curve fitting of the O 1s peak. It is believed that polyphosphates with different chain lengths have different mechanical and rheological properties [24], as a result of which the tribological performance can be affected. This method in determining the glass polymerisation number from the O 1s XPS peak has shown to give similar results when compared with other methods [32]. In figure 10, the polymerisation number (n) as a function of etching time is shown.

The accuracy of the O 1s XPS peak curve fitting was thought to be questionable [32,33] because of the linewidth of the peaks compared to the chemical shift. Hence in the analysis, first the linewidth of the peaks (FWHM) is determined and blocked to that value after which the curve fitting is performed. This procedure gives reliable information about the components formed.

Apparent from this analysis is the fact that the top layers of the tribofilms, formed from both lubricants, comprise Zn phosphate glass with similar chain length. The etching procedure shows that the 004A lubricant forms a phosphate glass with a higher chain length than the 002A lubricant. There were no oxides observed in the top layer of the 004A tribofilm, which is in agreement with other results [34].

5.2. Effect of ZDDP on MoDTC tribofilm formation

The Mo species that are found analysing the 003A and 004A tribofilms have binding energies of 228.2, 229.5, 231.6 and 232.2 eV. Knowing that binding energies 229.5 ± 0.3 eV and 232.2 ± 0.3 eV correspond to MoS₂ and Mo oxides, respectively, the detection of the Mo peak at 228.2 eV is interesting. It was thought that this peak occurs due to Ar etching and indeed control experiments on a MoS₂ powder, as shown in figure 11, confirmed this to be the case. With more etching no further shift of binding energy could be seen. Following the analysis on MoS₂ powder, it is concluded that the peak at 228.2 eV occurs as an etching effect of the MoS₂ peak.

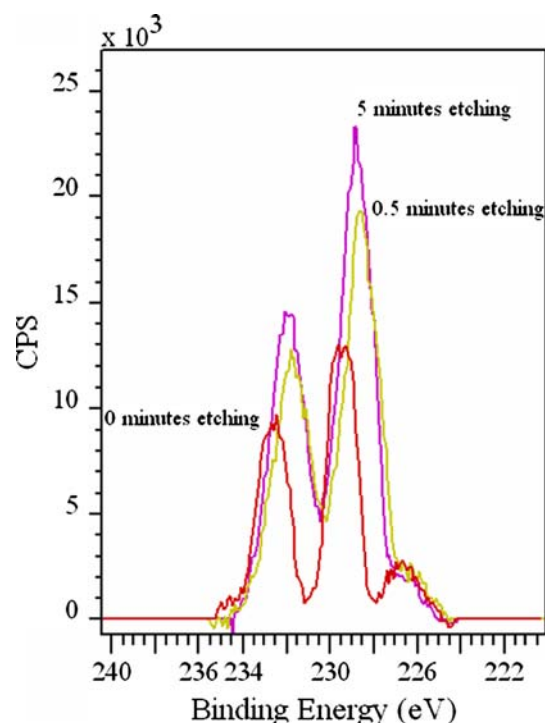


Figure 11. Mo3d peak obtained from scanning of MoS₂ powder after 0, 0.5 and 5 min etching.

Analysing the Mo 3d peak (figure 12 and table 6) it can be seen that in both tribofilms (003A and 004A), no Mo(V) (230.5 eV) peak is found. Since the Mo in

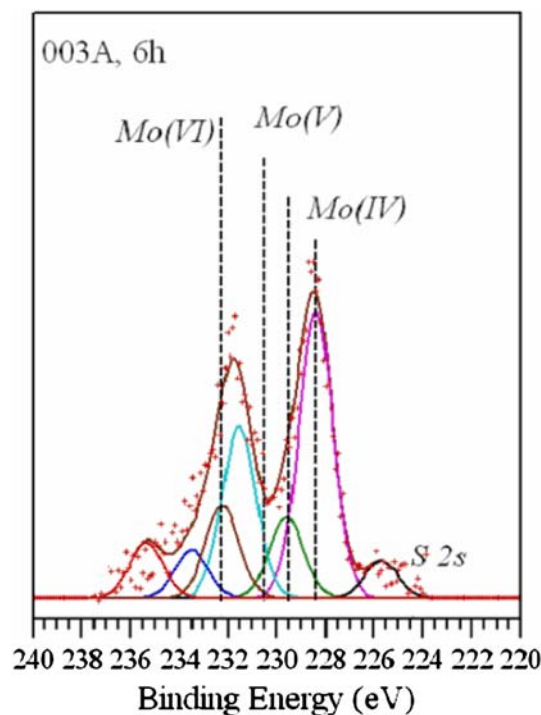


Figure 12. Mo3d peak curve fitting. The spectrum obtained from X-ray photoelectron spectroscopy (XPS) is shown with crosses.

MoDTC molecule has Mo(V) oxidation state, the absence of the Mo(V) peak, suggests that the MoDTC decomposition products deposit on the surface and not MoDTC itself.

In the literature, it is reported that ZDDP has a role in promoting the formation of MoS₂ on a surface from MoDTC. Surface analysis shows the formation of MoS₂ on both tribofilms, explaining effectiveness of both lubricants in friction reduction. This explains why they gave similar low friction and why the ANOVA statistical analysis did not show any interaction between ZDDP and MoDTC in affecting *final* friction. Consequently, the friction reduction does not seem to depend on the amount of MoS₂ in the overall tribofilm, which is in agreement with suggestion by Muraki *et al.* [31] that thickness of the MoS₂ tribofilm does not correspond directly to the friction. The interactions between ZDDP and MoDTC additives in film formation resulted in formation only of small amount of Mo phosphates.

The statistical analysis has been shown to be an effective way of identifying the main factors and interactions which have a significant effect on friction. But, the conclusions from ANOVA should be taken with consideration that they are factual only for the tests and friction values which are used in the analyses, in this case the friction value averaged from the last hour of the test.

5.3. Tribofilm evolution

From the analysis of the wear scar before and after the friction drop, it could be seen that in the case of the 003A lubricant no Mo species are found to be formed at the surface in the 30 min tests i.e. during the induction time. This is in agreement with results in Graham *et al.* [6] where Raman spectroscopy was used to analyse the chemical composition of the MoDTC tribofilms which gave high friction. They did not detect MoS₂ or molybdenum oxide in the wear scar. Graham *et al.* [6] suggested that the formation of the MoS₂ tribofilm might originate from an autocatalytic reaction i.e. chemical feedback, where the film once it starts to form, reduces wear of incipient MoS₂-forming species, which enables a fully efficient reaction film to start to develop.

In the case where 003A lubricant was used, the formation of FeS from MoDTC additive, shown earlier to form at the initial stage of tribofilm formation, will act as a protective layer reducing wear [35] and by that allowing the formation of a friction-reducing layer of MoS₂. AFM images (a and c) shown in figure 9, images that corresponds to MoDTC tribofilms in stages where the friction was high and reduced, do not show any significant change on structure, which is due to the presence of the C-rich layer identified from XPS quantification.

In the case where 004A lubricant was used, even after the 30-min test the formation of the ZDDP tribofilm

was seen. This can be seen both from the chemical analysis of the tribofilms and from AFM images (figure 9b, d). From curve fitting data of XPS peaks found in this tribofilm it was found that a similar ZDDP tribofilm to the 6-h test is formed. Aligned with the findings using the 003A lubricant, an N 1s peak was also seen, and with etching some Mo was detected. Despite the presence of ZDDP in the lubricant, the N organic group from the MoDTC molecule is found on the tribofilm. One of the suggestions as to the mechanism of the ZDDP effect would be that besides the formation of sulphides from the N group, the phosphate glass also serves as a wear-reducing layer to improving the conditions for the MoS₂ tribofilm to be formed and retained.

6. Conclusions

The effect of MoDTC and ZDDP tribofilm characteristics and their interactions in the tribofilm formation and the evolution of the tribofilms formed from MoDTC-containing lubricants are investigated. For the first time, a link between a theory of MoDTC additive chemical decomposition model and formed MoDTC tribofilm chemical characteristics obtained by the use of surface analytical techniques is made.

The main conclusions drawn from this work are given below:

- MoS₂ is detected in both tribofilms formed from MoDTC alone and in a blend with ZDDP explaining the low friction obtained when these lubricants were used.
- Prior to the formation of MoS₂ on the surface a FeS₂ is formed from the S in MoDTC molecule, which serves as a protective layer for retaining the MoS₂.
- In the case when ZDDP was used with MoDTC, beside FeS₂ and deposition of N organic layer, the phosphate layer was found to be formed. Both these species are known for their anti-wear properties, which by reducing wear make possible deposition of MoS₂ in the tribofilm.
- ZDDP/MoDTC lubricant gave higher wear than when ZDDP was used alone. This was linked to the lower amount of phosphate layer found on the tribofilm formed when ZDDP/MoDTC was used. Etching showed that ZDDP/MoDTC lubricant forms a phosphate film with higher chain length than the ZDDP one.

Acknowledgments

The authors would like to thank EPSRC, UK and Castrol Technology Centre, Pangbourne, UK for

financial support of this project. The authors are grateful to Dr. Graham Beamson from NCESS in Daresbury Laboratory, UK for assistance and discussion of the XPS results.

References

- [1] G.C. Smith, *J. Phys. D: Appl. Phys.* 33 (2000) R187–R197.
- [2] A.J. Gellman and N.D. Spencer, *Proc. Inst. Mech. Eng., Part J* 216 (2002) 443–461.
- [3] Y. Yamamoto and S. Gondo, *Tribol. Trans.* 32 (1989) 251–257.
- [4] F.A. Davis and T.S. Eyre, *Tribol. Int.* 23 (1990) 163–171.
- [5] J.M. Martin, T.L. Mogné, C. Grossiord and T. Palermo, *Tribol. Lett.* 2 (1996) 313–326.
- [6] J. Graham, H. Spikes and S. Korcek, *Tribol. Trans.* 44 (2001) 626–636.
- [7] J. Graham, H. Spikes and R. Jensen, *Tribol. Trans.* 44 (2001) 637–647.
- [8] C. Grossiord, K. Varlot, J.M. Martin, T.L. Mogné, C. Esnouf and K. Inoue, *Tribol. Int.* 31 (1998) 737–743.
- [9] A.R. Lansdown, *Molybdenum Disulphide Lubrication* (Elsevier, 1999).
- [10] M. Kasrai, J.N. Cutler, K. Gore, G. Canning and G.M. Bancroft, *Tribol. Trans.* 41 (1998) 69–77.
- [11] M. Muraki, Y. Yanagi and K. Sakaguchi, *Tribol. Int.* 30 (1997) 69–75.
- [12] R. Unnikrishnan, M.C. Jain, A.K. Harinarayan and A.K. Mehta, *Wear* 252 (2002) 240–249.
- [13] J.M. Martin, T.L. Mogné, M. Boehm and C. Grossiord, *Tribol. Int.* 32 (1999) 617–626.
- [14] J.M. Martin, C. Crossiord, K. Varlot, B. Vacher and J. Igarashi, *Tribol. Lett.* 8 (2000) 193–201.
- [15] G.W. Stachowiak and A.W. Batchelor, *Engineering Tribology* (Butterworth-Heinemann, 2001).
- [16] D.C. Montgomery, *Design and Analysis of Experiments* (John Wiley & Sons, Inc, New York, 1997).
- [17] R.H. Lochner and J.E. Matar, *Designing for Quality* (Chapman & Hall, London, 1990), p. 42.
- [18] G. Beamson and D. Briggs, *High Resolution XPS of Organic Polymers, The Scienta ESCA300 Database* (Wiley, Chichester, 1992).
- [19] N. Fairley, CasaXPS Version 2.1.25.
- [20] J.F. Moulder, W.F. Stickle, P.E. Sobol and K.D. Bomben, *Handbook of X-ray Photoelectron Spectroscopy* (Pelmir-Elmer Corporation, Minnesota, 1992).
- [21] E.C. Onyiriuka, *J. Non-Cryst. Solids* 163 (1993) 268–273.
- [22] S.O. Grim, L. Matienzo, *Inorg. Chem.* 14 (1975) 1014–1018.
- [23] A. Morina, J. Green, A. Neville and M. Priest, *Tribol. Lett.* 15 (2003) 443–452.
- [24] J.M. Martin, C. Grossiord, T.L. Mogné, S. Bec and A. Tonck, *Tribol. Int.* 34 (2001) 523–530.
- [25] A. Morina, J.H. Green, A. Neville and M. Priest, *Additive/additive Interactions in Boundary Lubrication – a Study of Film Formation and Tenacity, Life Cycle Tribology, Proc. 31st Leeds-Lyon Symposium on Tribology, Leeds 2004, Tribology and Interface Engineering Series* (Elsevier, Amsterdam, 2005), pp. 757–767.
- [26] C.D. Wagner, A.V. Naumkin, A. Kraut-Vass, J.W. Allison, C.J. Powell, J.R.R. Jr., *NIST Standard Reference Database 20, Version 3.4 (Web Version)* <http://www.srdata.nist.gov/xps/> (2003).
- [27] M. Aktary, M.T. McDermott and J. Torkelson, *Wear* 247 (2001) 172–179.
- [28] A.J. Pidduck and G.C. Smith, *Wear* 212 (1997) 254–264.
- [29] J. Ye, M. Kano and Y. Yasuda, *Tribol. Lett.* 13 (2002) 41–47.
- [30] L.J. Taylor and H.A. Spikes, *Tribol. Trans.* 46 (2003) 303–309.
- [31] M. Muraki and H. Wada, *Jpn. J. Tribol.* 38 (1993) 1347–1359.
- [32] C. Minfray, J.M. Martin, C. Esnouf, T.L. Mogné, R. Kersting and B. Hagenhoff, *Thin Solid Films* 447 (2004) 272–277.
- [33] J.M. Martin, *Tribol. Lett.* 6 (1999) 1–8.
- [34] C. Grossiord, J.M. Martin and T.L. Mogné, *J. Vac. Sci. Technol. A* 17 (1999) 884–890.
- [35] E.S. Forbes, *Wear* 15 (1970) 87–96.